Infection and Drug Resistance

Dovepress
open access to scientific and medical research

Open Access Full Text Article

ORIGINAL RESEARCH

Genetic Characterization of Four Groups of Chromosome-Borne Accessory Genetic Elements Carrying Drug Resistance Genes in *Providencia*

Jiayao Guan[1,*], Chunmei Bao[2,*], Peng Wang[3], Ying Jing[3], Lingling Wang[3], Xinyue Li[3], Xiaofei Mu[3], Boan Li[2], Dongsheng Zhou[3], Xuejun Guo[1], Zhe Yin[3]

[1]Key Laboratory of Jilin Province for Zoonosis Prevention and Control, Changchun Veterinary Research Institute, Chinese Academy of Agricultural Sciences, Changchun, Jilin, 130122, People's Republic of China; [2]Fifth Medical Center of Chinese PLA General Hospital, Beijing, 100039, People's Republic of China; [3]State Key Laboratory of Pathogen and Biosecurity, Beijing Institute of Microbiology and Epidemiology, Beijing, 100071, People's Republic of China

*These authors contributed equally to this work

Correspondence: Zhe Yin, State Key Laboratory of Pathogen and Biosecurity, Beijing Institute of Microbiology and Epidemiology, Beijing, 100071, People's Republic of China, Tel +86-10-66948557, Email jerry9yin@163.com; Xuejun Guo, Key Laboratory of Jilin Province for Zoonosis Prevention and Control, Changchun Veterinary Research Institute, Chinese Academy of Agricultural Sciences, Changchun, Jilin, 130122, People's Republic of China, Tel +86-431-86985931, Email xuejung2021@163.com

Purpose: The aim of this study was to gain a deeper genomics and bioinformatics understanding of diversification of accessory genetic elements (AGEs) in *Providencia*.

Methods: Herein, the complete genome sequences of five *Providencia* isolates from China were determined, and seven AGEs were identified from the chromosomes. Detailed genetic dissection and sequence comparison were applied to these seven AGEs, together with additional 10 chromosomal ones from GenBank (nine of them came from *Providencia*).

Results: These 17 AGEs were divided into four groups: Tn*6512* and its six derivatives, Tn*6872* and its two derivatives, Tn*6875* and its one derivative, and Tn*7* and its four derivatives. These AGEs display high-level diversification in modular structures that had complex mosaic natures, and particularly different multidrug resistance (MDR) regions were presented in these AGEs. At least 52 drug resistance genes, involved in resistance to 15 different categories of antimicrobials and heavy metal, were found in 15 of these 17 AGEs.

Conclusion: Integration of these AGEs into the *Providencia* chromosomes would contribute to the accumulation and distribution of drug resistance genes and enhance the ability of *Providencia* isolates to survive under drug selection pressure.

Keywords: *Providencia*, integrative and conjugative elements, integrative and mobilizable elements, unit transposons, multidrug resistance

Introduction

Providencia species, mostly frequently identified as *Providencia rettgeri* and *Providencia stuartii*, are opportunistic pathogens causing urinary tract infections, diarrhea, and bacteremia in immunocompromised patients.[1] *Providencia* is intrinsically resistant to penicillins and the first-generation cephalosporins due to inducible expression of AmpC β-lactamases,[2] aminoglycosides by the reason of inducible expression of AAC(2')-Ia,[3] tetracyclines because of constitutive expression of a multidrug efflux pump AcrAB,[4] and polymyxins resulting from the presence of a cell envelop that inhibits colistin to combine with the susceptible lipid target sites or the lipid A modification to reduce binding.[5] In recent years, the wide use of aminoglycosides, β-lactams, and fluoroquinolones for antimicrobial therapy aggravates the acquisition and dissemination of diverse antimicrobial resistance genes in *Providencia*.[6] Acquired antimicrobial

Received: 8 February 2022
Accepted: 20 April 2022
Published: 27 April 2022

resistance genes in *Providencia* are commonly captured and horizontally transferred by accessory genetic elements (AGEs), such as integrative and conjugative elements (ICEs), integrative and mobilizable elements (IMEs), and unit transposons.

ICEs have the ability to transfer from one cell to another cell through conjugation and are autonomous in conjugation by mainly utilizing a type IV secretion system (T4SS) and a coupling protein.[7] Up to now, three distinct families of ICEs, namely Tn*6512* (R391),[8] ICE*Ec2*,[9] and ICE*Pm1*[10] have been reported in *Providencia*. Tn*6512* is initially found in *Providencia rettgeri* in 1972,[8] and since then a wealth of Tn*6512*-related ICEs have been identified in not only *Providencia*,[8,11] but also Enterobacteriaceae,[12] Vibrionaceae,[13] *Shewanella*,[14] *Actinobacillus*,[15] *Alteromonas*,[16] *Pseudoalteromonas*.[17] Tn*6512*-related ICEs carry at least five hotspots (located within the intragenic or intergenic sites of their backbone regions) for integration of foreign resistance genes,[18] which causes these ICEs being mosaic and diversified with respect to their modular structures.

IMEs do not encode the T4SS machinery and the coupling protein and thus is nonautonomous in conjugation.[19] The conjugal transfer of an IME from a donor cell into a recipient cell relies on the T4SS gene sets of a helper conjugative element such as an IncA/C conjugative plasmid.[20] So far, three distinct families of IMEs, namely Tn*6523* (SGI1),[21] Tn*6588*,[22] and Tn*6591*[22] have been reported in *Providencia*.

ICEs and IMEs can be transferred in an intercellular manner, while the Tn*7*-family unit transposons use a "cut-and-paste" transposition mechanism to transfer intracellularly, which is typically promoted by the core transposition determents TnsA (endonuclease), TnsB (transposase), TnsC (transposition regulator), and TnsD plus TnsE (target-site selection proteins).[23] Tn*7*-family transposons have widely been found as the vectors of diverse antimicrobial resistance genes in Morganellaceae including *Providencia rettgeri*,[22] Enterobacteriaceae,[24] Pseudomonadaceae,[25] Burkholderiaceae,[26] *Acinetobacter*,[27] *Shewanella*,[24] *Hahella*,[24] *Pelobacter*,[24] *Idiomarina*,[24] *Acidithiobacillus*,[24] *Neisseria* (eg *N. brasiliensis* with an accession number CP046027), *Nitrosomonas* (eg *N. stercoris* with an accession number AP019755), and *Bacillus*.[24]

This study presented the complete sequences of seven chromosome-borne AGEs in five sequenced *Providencia* isolates from China. Detailed genetic dissection and comparison were applied to these seven AGEs, together with additional 10 chromosome-borne ones from GenBank (nine of them came from *Providencia*). These 17 AGEs could be classified into ICEs, IMEs, and Tn*7* derivatives. Data presented here provided a deeper genomics and bioinformatics understanding of diversification of AGEs in *Providencia*.

Materials and Methods

Providencia rettgeri PROV275, PROV002, and PROV087 (Table S1) causing nosocomial infections were recovered from three different Chinese public hospitals in 2014, 2013, and 2016, respectively. *Providencia alcalifaciens* PROV023 and PROV013 (Table S1) were collected from two different China livestock farms in 2017. Whole-genome sequencing of these five *Providencia* isolates were conducted with a sheared DNA library with average size of 15 kb (ranged from 10 kb to 20 kb) on a PacBio RSII sequencer (Pacific Biosciences, CA, USA) and further sequence data mining was performed as described previously.[28] The sequencing data was conducted using NanoPack[29] and FastQC (https://www.bioinformatics.babraham.ac.uk/projects/fastqc) (Table S2). Conjugal transfer of Tn*6862* from the wild-type PROV023 isolate into the rifampin-resistant recipient strain *Escherichia coli* EC600 was performed as described previously.[30] Bacterial antimicrobial susceptibility was tested by BioMérieux VITEK 2, and interpreted as per the 2020 Clinical and Laboratory Standards Institute (CLSI) guidelines.[31] The antimicrobial drug susceptibility profiles of the five *Providencia* isolates, EC600, and the transconjugant was shown in Table S3. All the wild-type and transconjugant strains were subjected to PCR amplification followed by amplicon sequencing, for determining the sequences of bacterial 16S rDNA, the presence of key markers such as *aphA1, strA, strB, int*, and *cpl*, and also the location/boundary of AGEs such as Tn*6860*, Tn*6861*, Tn*6862*, Tn*6873*, and Tn*6876* (data not shown). The complete chromosome sequences of the PROV275, PROV002, PROV023, PROV013, and PROV087 isolates were submitted to GenBank under accession numbers CP059298, CP059345, CP059348, CP059346, and CP059347, respectively. The GenBank accession numbers of all the six plasmids of these five isolates were listed in Table S1.

Results

Four Groups of 17 Chromosome-Borne AGEs

In this study, the complete genome sequences from *Providencia rettgeri* PROV275, PROV002, and PROV087 and *Providencia alcalifaciens* PROV023 and PROV013 were determined, and then a total of seven chromosome-borne AGEs were identified: i) Tn*6860*, Tn*6861*, and a 102.1-kb Tn*7*-related element $T7RE_{PROV087}$ from strains PROV275, PROV002, and PROV087, respectively; ii) Tn*6862* and a 35.9-kb $T7RE_{PROV023}$ from strain PROV023; and iii) Tn*6873* and Tn*6876* from strain PROV013. Then, a detailed sequence comparison was applied to a collection of four groups of 17 chromosome-borne AGEs (16 of them from *Providencia*): i) seven related ICEs Tn*6512*,[8] Tn*6860*, Tn*6861*, Tn*6862*, Tn*6863*,[18] Tn*6864*,[11] and Tn*6865*; ii) three related IMEs Tn*6872*, Tn*6873*, and Tn*6874*; iii) two related IMEs Tn*6875* and Tn*6876*; and iv) Tn*7* and its four derivatives $T7RE_{PROV087}$, $T7RE_{PROV023}$, a 58.0-kb $T7RE_{MF1}$, and a 40.7-kb $T7RE_{Pr\text{-}15\text{-}2\text{-}50}$ (Table 1). At least 52 drug resistance genes, involved in resistance to 15 different categories of antimicrobials and heavy metal, were identified in 15 (expect for Tn*6872* and Tn*6875*) of these 17 AGEs (Figure 1 and Table S4). All of these T7RE, T1696RE (see below), and T21RE (see below) elements could not be recognized as intact transposons due to truncation of relevant core transposition modules.

Six Tn6512-Related ICEs Tn6860, Tn6861, Tn6862, Tn6863, Tn6864, and Tn6865

All these seven ICEs including Tn*6512* were integrated into the same 17-bp target site located within the 5' end of the chromosomal gene *prfC* (peptide chain release factor 3).[32] These seven ICEs (Figure S1) had similar conserved backbones,[33] containing *int* (integrase), *xis* (excisionase), *rlx* (relaxase), *oriT* (origin of conjugative replication), *cpl* (coupling protein), a TivF-type T4SS gene set, and *attL*/*R* (attachment sites at the left/right end). A toxin-antitoxin system was encoded by each of the five ICEs (*hipBA* in Tn*6512*, and *abiEi–ii* in Tn*6860*, Tn*6861*, Tn*6863*, and Tn*6864*) except for Tn*6862* and Tn*6865*. Type I restriction-modification system *hsdMSR* was carried by five of them except for Tn*6512* and Tn*6865*.

The major modular differences were recognized at least 10 regions/sites (Figure 2 and Table S5) across the whole genomes of these seven ICEs. Firstly, a total of 23 events of acquisition of exogenous DNA region occurred at nine regions/sites within these seven ICEs. Secondly, a total of 12 events of backbone region deletion (10 of them were resulted from acquisition of exogenous DNA region) occurred at five regions/sites within these seven ICEs. Finally, totally 21 events of substitution of backbone region occurred at four regions/sites within six ICEs.

Each of these seven ICEs carried two to five accessory modules (Figure S1), including multidrug resistance (MDR) regions, composite transposons, IME, integron, insertion sequence (IS) elements, and so called "inserted regions". Firstly, the 33.5-kb, 62.0-kb, 29.8-kb, 14.2-kb, 18.3-kb, and 33.0-kb MDR regions were integrated at the same site within Tn*6860*, Tn*6861*, Tn*6862*, Tn*6863*, Tn*6864*, and Tn*6865*, respectively. Secondly, an IS*15DI* (a minor variant of IS*26*)-composite transposon Tn*6578* (containing *aphA1*), an IME Tn*6912* (containing $bla_{HMS\text{-}1}$), and an IS*Ppu12*-composite transposon Tn*6896* were inserted into the different sites within Tn*6512*, Tn*6860*, and Tn*6864*, respectively. Tn*6896* (Figure 3) was bracketed by 8-bp direct repeats (DRs; target site duplication signals for transposition), and carried *tetA* (C)-carrying ΔTn*6309*, and a concise class 1 integron In525 with the gene cassette array (GCA) *aadA2–ereA–dfrA32*. Thirdly, a class 9 integron In9-1 (containing *dfrA1*) was inserted within Tn*6863*. Finally, multiple IS elements and inserted regions were found at the different sites within these ICEs.

These six MDR regions (Figure 4) shared only a 0.5-kb Tn*3*-family Tn remnant together with an IS*Shfr9* element, and they carried dramatically different profiles of resistance loci. The 33.5-kb MDR region carried three resistance loci: a truncated IS*CR2–floR* unit, a 12.6-kb region (containing $bla_{CTX\text{-}M\text{-}3}$-carrying ΔTn*6502a*) from IncM plasmid R69,[34] and IS*Ec29–mph*(E)–IS*15DI* unit. The 62.0-kb MDR region was composed of five resistance loci: a 23.4-kb Tn*1696*-related element $T1696RE_{PROV002}$ (see below), *tetA*(C)-carrying Tn*6309*, a concise class 1 integron In1793 (GCA: *gacG2–aadA6–gacG2*), a truncated IS*26–mph*(A)–IS*6100* unit, and *mer* region. The 29.8-kb, 14.2-kb, and 18.3-kb MDR regions shared a truncated IS*CR2–sul2* unit (containing *strAB*-carrying ΔTn*5393c*), but each of them integrated one or two additional resistance loci: i) an interrupted IS*CR2–floR* unit and an IS*1006*-composite transposon Tn*6976* (which was bracketed by 5-bp DRs and contained two resistance loci: *aphA1*-carrying ΔTn*4352* and IS*26–aacC4–aph*

Table 1 Major Features of the 17 AGEs Characterized in This Work

Group	Accessory Genetic Element	Accession Number	Chromosomal Nucleotide Position	Length (bp)	Host Bacterium	Reference
Tn*6512*-related ICEs	Tn*6512*	AY090559	Not applicable	88,549	*Providencia rettgeri* 107	8
	Tn*6860*	CP059298	575696.691964	116,269	*Providencia rettgeri* PROV275	This study
	Tn*6861*	CP059345	727272.869956	142,685	*Providencia rettgeri* PROV002	This study
	Tn*6862*	CP059348	704853.810761	105,909	*Providencia alcalifaciens* PROV023	This study
	Tn*6863*	GQ463139	Not applicable	96,586	*Providencia alcalifaciens* Ban1	18
	Tn*6864*	MT219827	Not applicable	107,207	*Providencia rettgeri* RF14-2	11
	Tn*6865*	CP031123	751328.820050	68,723	*Providencia huaxiensis* WCHPr000369	Not applicable
Tn*6872*-related IMEs	Tn*6872*	LR134189	025117.3045606	20,490	*Providencia rustigianii* NCTC6933	Not applicable
	Tn*6873*	CP059346	2973270.3043055	69,786	*Providencia alcalifaciens* PROV013	This study
	Tn*6874*	AP022371	3358722.3420122	61,401	*Providencia rettgeri* BML2496	Not applicable
Tn*6875*-related IMEs	Tn*6875*	CP031508	1032159.1038038	5880	*Providencia stuartii* FDAARGOS_87	Not applicable
	Tn*6876*	CP059346	2583916.2605820	21,905	*Providencia alcalifaciens* PROV013	This study
Tn*7*-related elements	Tn*7*	KX117211	Not applicable	14,067	*Escherichia coli* 3.5-R3	47
	102.1-kb T7RE$_{PROV087}$	CP059347	33162.135304	102,143	*Providencia rettgeri* PROV087	This study
	35.9-kb T7RE$_{PROV023}$	CP059348	47906.83831	35,926	*Providencia alcalifaciens* PROV023	This study
	58.0-kb T7RE$_{MF1}$	CP048621	1077700.1135740	58,041	*Providencia stuartii* MF1	Not applicable
	40.7-kb T7RE$_{Pr-15-2-50}$	CP039844	31494.72272	40,779	*Providencia rettgeri* Pr-15-2-50	Not applicable

(4)-Ia–IS*Ec59* unit) in 29.8-kb MDR region; ii) IS*CR2–floR* unit in 14.2-kb MDR region; and iii) IS*CR2–erm42* unit and a truncated IS*CR2–tet*(X6) unit in 18.3-kb MDR region. The 33.0-kb MDR region had the sole resistance locus In1571, whose 5'-conserved segment (5'-CS: *intI–attI1*) was interrupted by IS*26*. In1571 was a complex class 1 integron, which contained two resistance loci: GCA (also called VR1: variable region 1) *fosC2–aacA4'-8–ereA1e–bla*$_{OXA-21}$*–dfrA1r*, and VR2 composed of IS*CR1–qnrVC1* unit and a truncated IS*CR1–bla*$_{PER-4}$ unit.

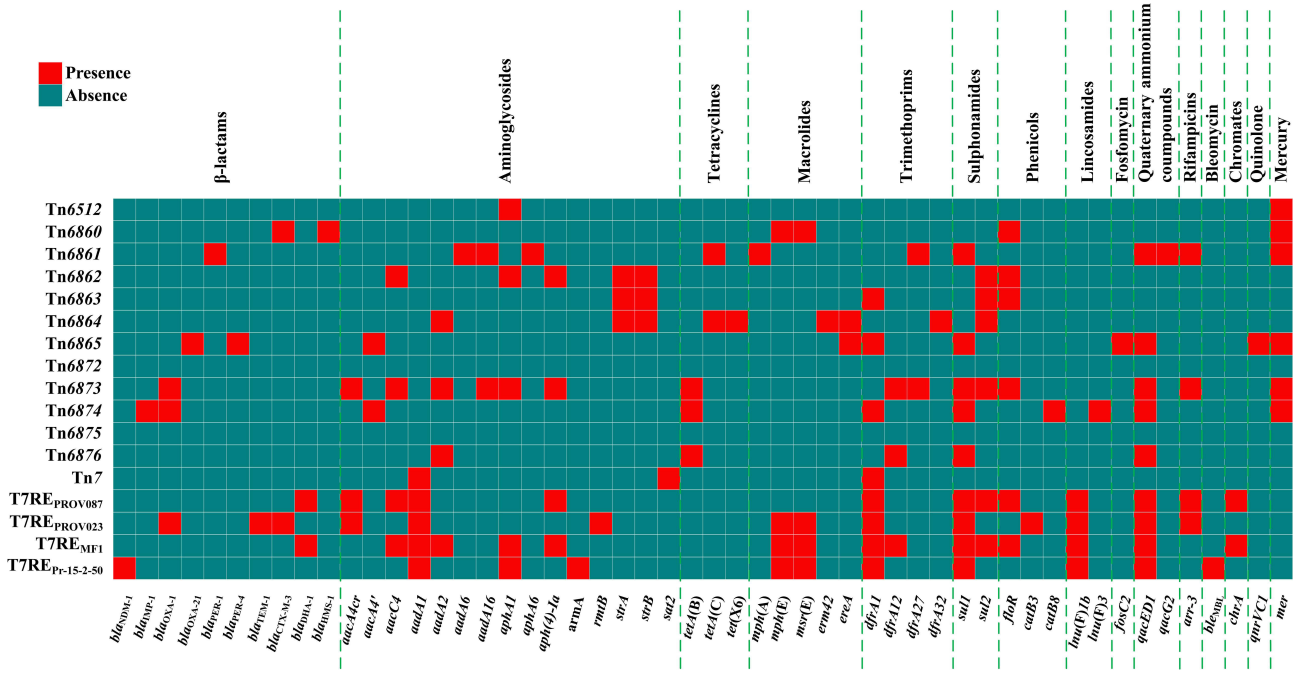

Figure 1 Heatmap of prevalence of drug resistance genes.
Notes: Original data are shown in Table S4.

*Three Related IMEs Tn*6872, *Tn*6873, *and Tn*6874

All these three IMEs were integrated 102-bp upstream the chromosomal gene *mutS* (DNA mismatch repair protein). The prototype IME Tn*6872* was initially found in *Providencia rustigianii* NCTC6933 (accession number LR134189). These three IMEs (Figure 5) shared the core IME backbone markers *int, oriT* and *attL*/*R*. Tn*6872* harbored its three unique backbone regions *orf201*–to–*orf207, orf627*–to–*orf1068*, and *orf1338*–to–*uvrD*; correspondingly, Tn*6873*/Tn*6874* carried their unique backbone regions *hsdMSR* (type I restriction-modification system)–*mrr*–*orf411, orf597*–to–*orf1107*, and *orf1311*–to–*hnhc*, instead of the above three Tn*6872*-unique regions, respectively. No accessory modules were found in Tn*6872*, but a 47.0-kb MDR region and a 38.5-kb MDR region were integrated at the same site within Tn*6873* and Tn*6874*, respectively.

The 47.0-kb MDR region (Figure 6) contained six resistance loci: a concise class 1 integron In27 (GCA: *dfrA12*–*gcuF*–*aadA2*), ΔTn*4352* containing *aphA1*, IS*26*–*aph(4)-Ia*–*aacC4*–IS*Ec59* unit, IS*CR2*–*sul2* unit, a truncated IS*CR2*–*floR* unit, and a Tn*21*-related transposon Tn*6974* (see below). The 38.5-kb MDR region carried an IME Tn*6977*, and a Tn*1696*-related transposon Tn*6910* (see below).

*Two Related IMEs Tn*6875 *and Tn*6876

Tn*6875* and Tn*6876* were integrated 494-bp downstream the chromosomal gene *smpB* (SsrA-binding protein). The prototype IME Tn*6875* was initially found in *Providencia stuartii* FDAARGOS_87 (accession number CP031508). Tn*6875* and Tn*6876* (Figure 7) shared the core IME backbone markers *int* and *attL*/*R*, but they displayed two major modular variations: i) Tn*6875* contained its unique backbone region *rimI*–to–*orf567*, while Tn*6876* harbored its unique backbone region containing *orf288*; and ii) Tn*6875* carried no accessory modules, but Tn*6876* acquired a 20.0-kb MDR region composed of *tetA*(B)-containing Tn*10* and 10.4-kb T1696RE$_{PROV013}$ (see below).

Four *Tn7* Derivatives *T7RE*$_{PROV087}$,*T7RE*$_{PROV023}$, *T7RE*$_{MF1}$, *and T7RE*$_{Pr-15-2-50}$

Tn*7* and its three derivatives T7RE$_{PROV087}$, T7RE$_{PROV023}$, and T7RE$_{Pr-15-2-50}$ were inserted 25-bp downstream of the chromosomal gene *glmS* (glutamine-fructose-6-phosphate aminotransferase), while the remaining one T7RE$_{MF1}$ was inserted within the chromosomal gene *orf1389* (carbohydrate porin). T7RE$_{PROV087}$, T7RE$_{PROV023}$, T7RE$_{MF1}$, and

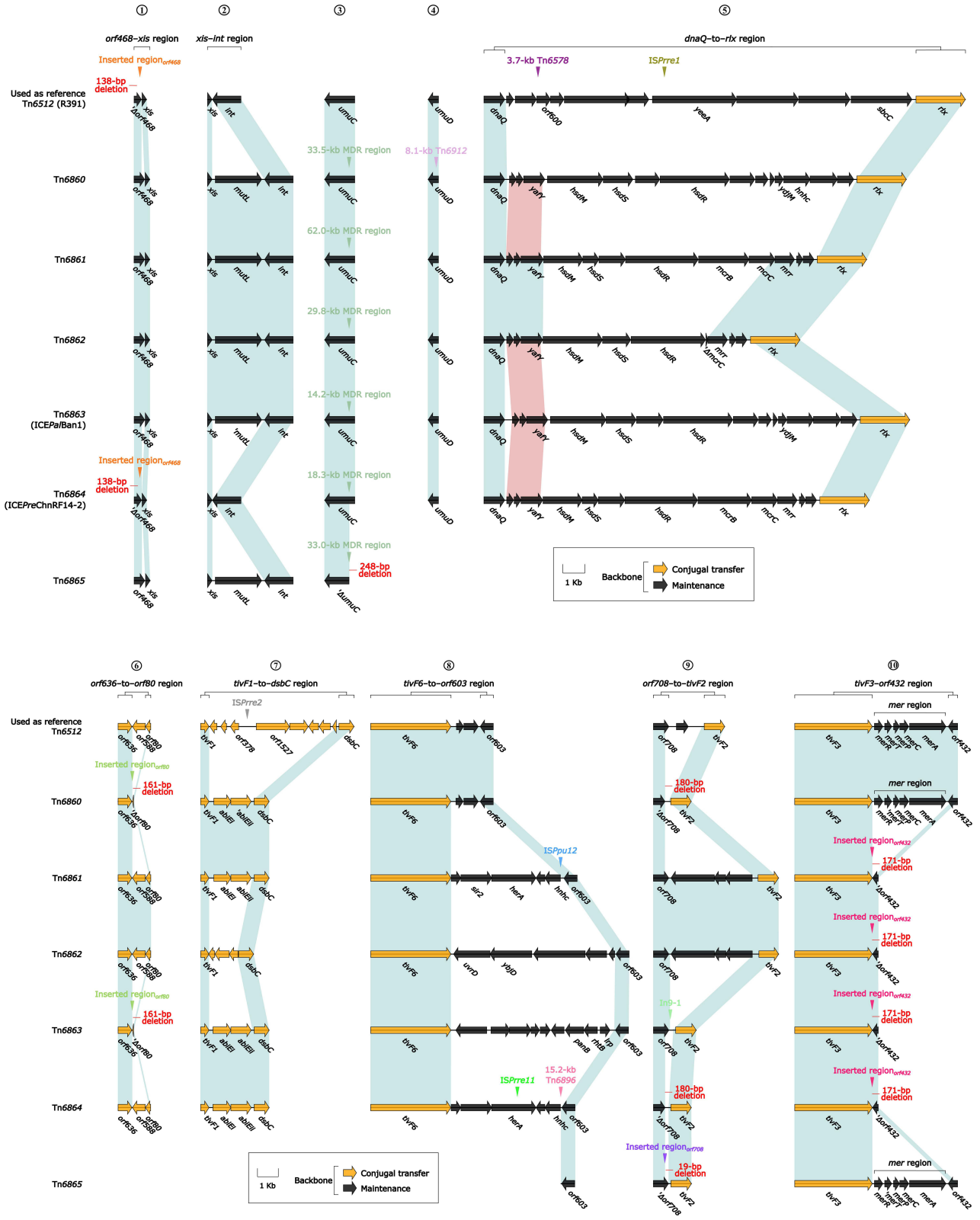

Figure 2 Massive gene acquisition and loss across whole-genomes of seven related ICEs Tn*6512*, Tn*6860*, Tn*6861*, Tn*6862*, Tn*6863*, Tn*6864*, and Tn*6865*.
Notes: Genes are denoted by arrows. Genes, AGEs, and other features are colored based on their functional classification. Shading in light blue or light orange denotes regions of homology (nucleotide identity ≥90%), light pink (nucleotide identity <90%). The seven Tn*6512*-related ICEs are listed at vertical coordinates, while the 10 genomic regions/sites (numbers in circles) with major modular differences (for details in Table S5) are shown at horizontal coordinates. Please also refer to the detailed genetic organization of the accessory modules inserted within regions 1, 5, 6, 7, 9, and 10, plus site 4 (Figure S1), site 3 (Figure 4), and region 8 (Figures 3 and S1).

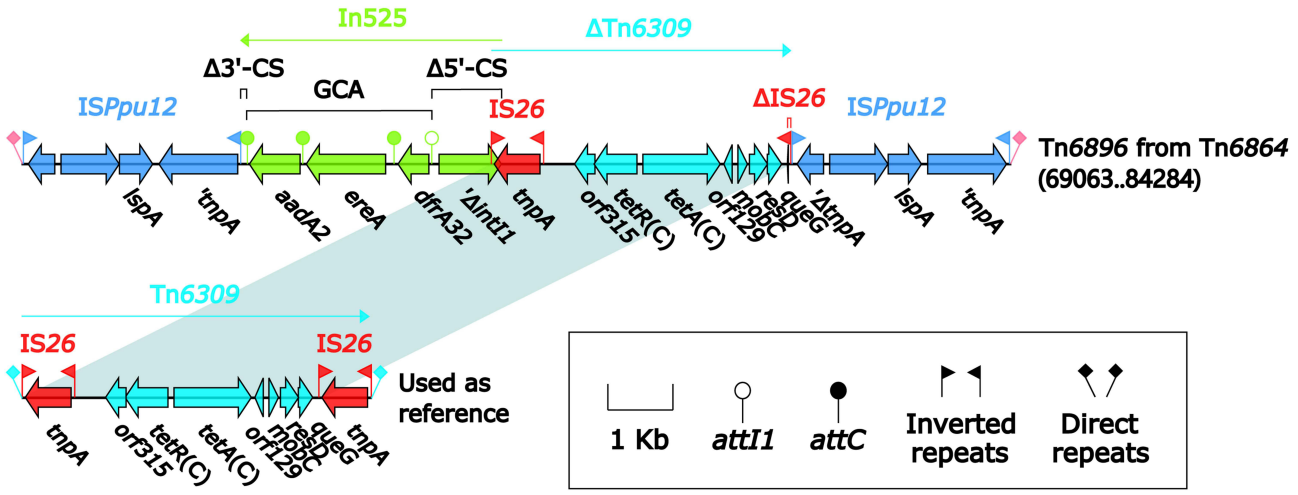

Figure 3 Organization of Tn*6896* from Tn*6864*, and comparison to related regions.
Notes: Genes are denoted by arrows. Genes, AGEs, and other features are colored based on their functional classification. Shading in light blue denotes regions of homology (nucleotide identity ≥95%). Numbers in brackets indicate nucleotide positions within Tn*6864*. Accession number of Tn*6309*[48] used as reference is KX710094.

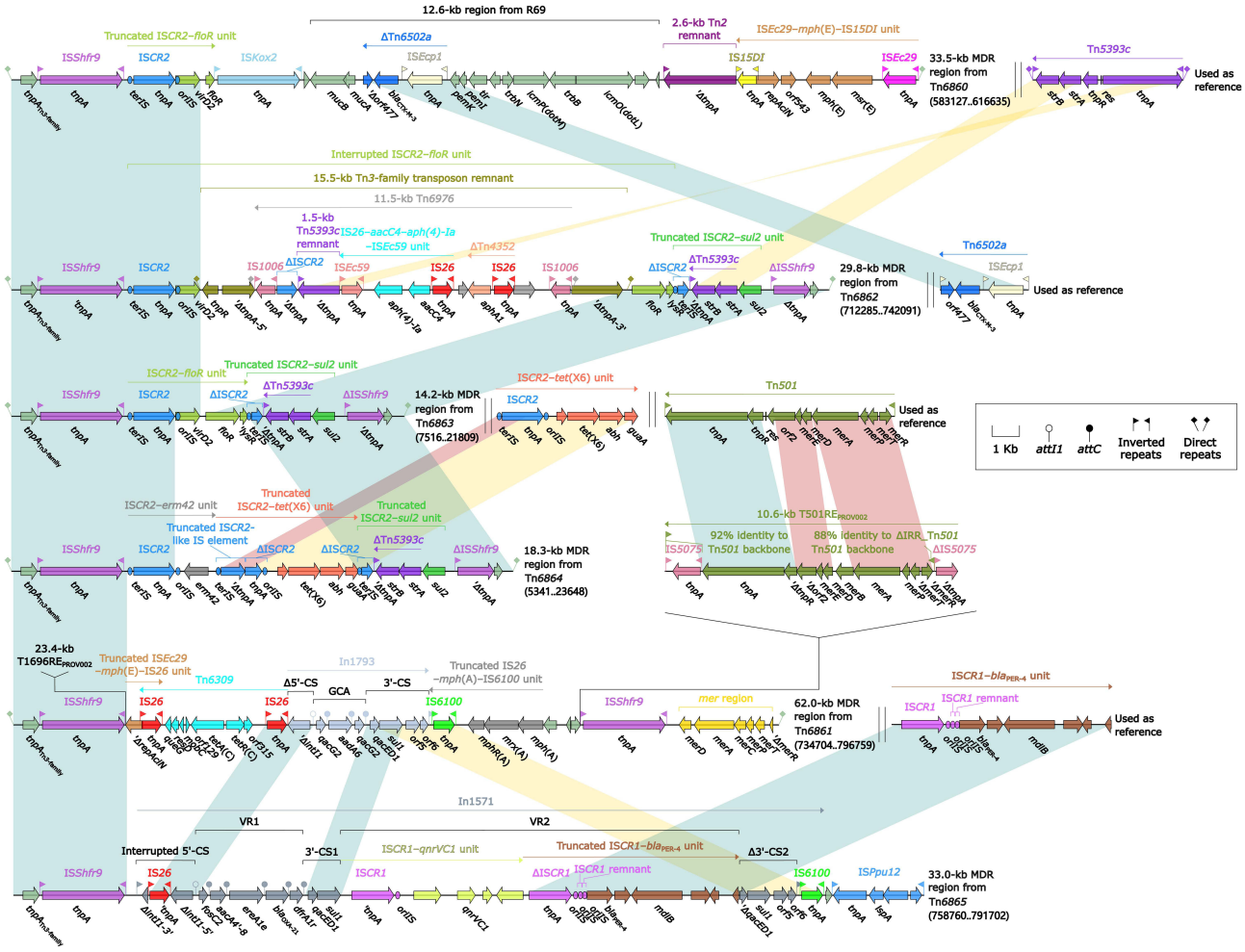

Figure 4 Comparison of MDR regions from Tn*6860*, Tn*6861*, Tn*6862*, Tn*6863*, Tn*6864*, and Tn*6865*.
Notes: Genes are denoted by arrows. Genes, AGEs, and other features are colored based on their functional classification. Shading in light blue or light orange denotes regions of homology (nucleotide identity ≥90%), light pink (nucleotide identity <90%). Numbers in brackets indicate nucleotide positions within the chromosomes of strains PROV275 and PROV023, Tn*6863*, Tn*6864*, and the chromosomes of strains PROV002 and WCHPr000369, respectively. Accession numbers of ISCR*1*–*bla*PER-4 unit,[49] Tn*6502a*,[50] Tn*501*,[51] ISCR*2*–*tet*(X6) unit,[11] and Tn*5393c*[52] used as reference are KU133341, KF914891, Z00027, CP047340, and AF262622, respectively.

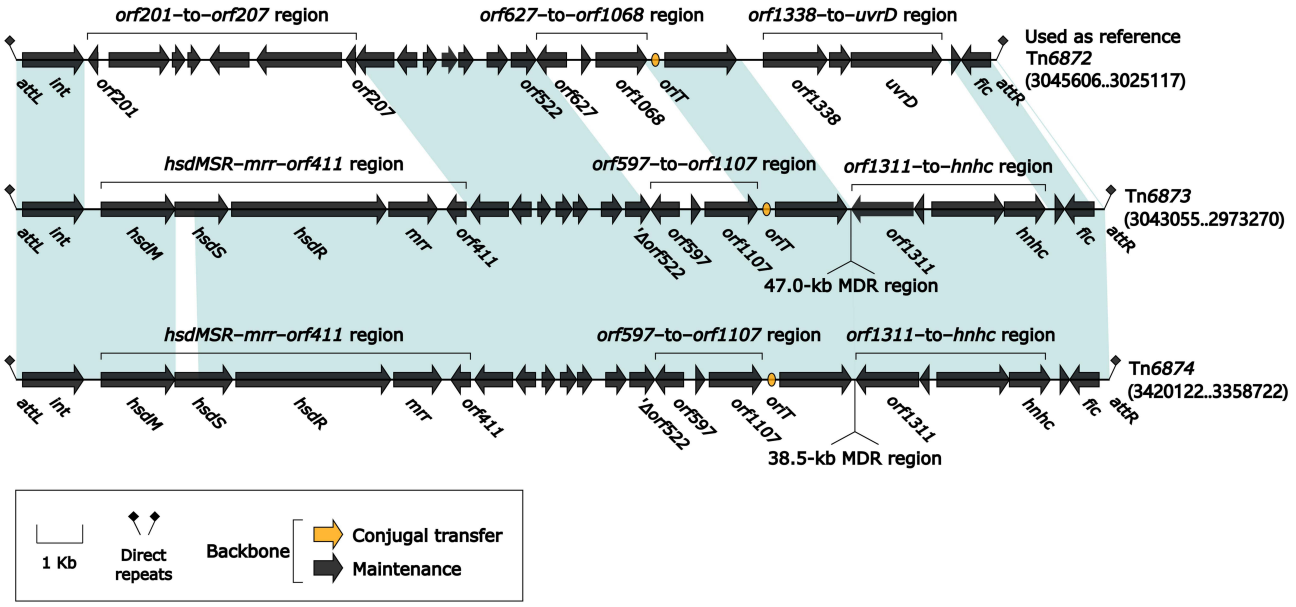

Figure 5 Comparison of three related IMEs Tn*6872*, Tn*6873*, and Tn*6874*.
Notes: Genes are denoted by arrows. Genes, AGEs, and other features are colored based on their functional classification. Shading in light blue denotes regions of homology (nucleotide identity ≥90%). Numbers in brackets indicate nucleotide positions within the chromosomes of strains NCTC6933, PROV013, and BML2496, respectively. Accession number of Tn*6872* used as reference is LR134189.

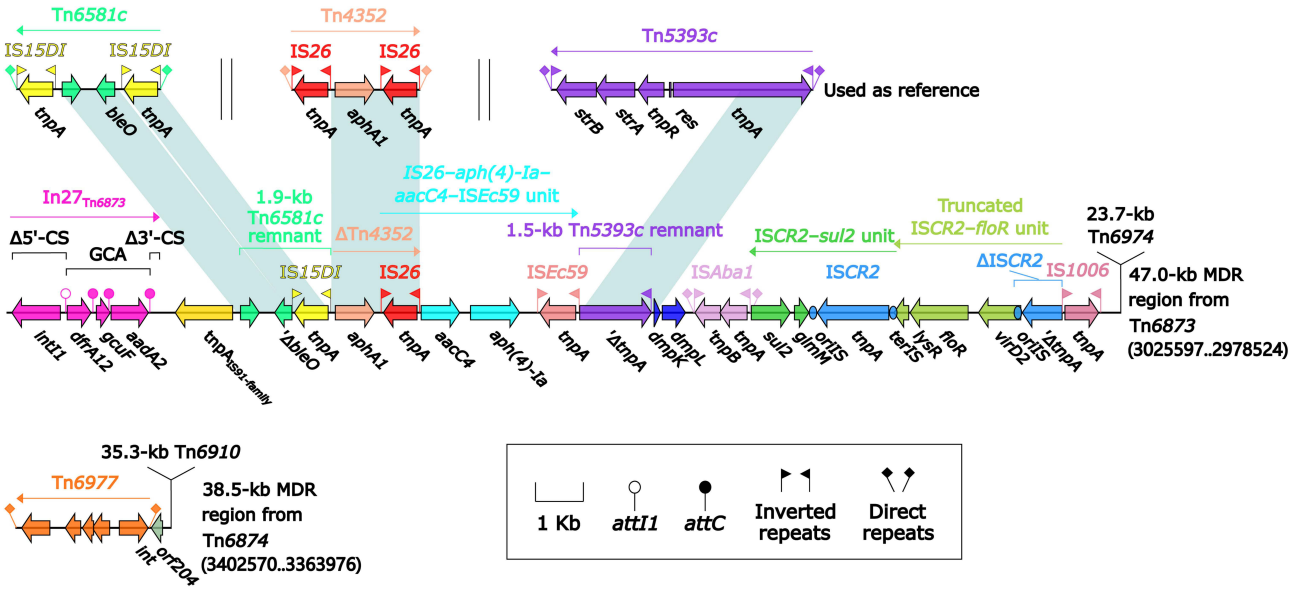

Figure 6 Organization of MDR regions from Tn*6873* and Tn*6874*, and comparison to related regions.
Notes: Genes are denoted by arrows. Genes, AGEs, and other features are colored based on their functional classification. Shading in light blue denotes regions of homology (nucleotide identity ≥95%). Numbers in brackets indicate nucleotide positions within the chromosomes of strains PROV013 and BML2496, respectively. Accession numbers of Tn*6581c*,[22] Tn*4352*,[53] and Tn*5393c*[52] used as reference are CO042857, CP04285, and AF262622, respectively.

T7RE$_{Pr\text{-}15\text{-}2\text{-}50}$ (Figure 8) differed from Tn*7* by acquisition of 95.9-kb, 29.7-kb, 51.8-kb, and 33.6-kb MDR regions, respectively, instead of In2-4 (GCA: *dfrA1–sat2–aadA1*). The above acquisition events resulted in the same truncation of *tnsABCDE* in these four Tn*7* derivatives. Moreover, *tnsB* of T7RE$_{Pr\text{-}15\text{-}2\text{-}50}$ was interrupted by insertion of IS*Prst3*.

These four MDR regions (Figure 9) shared only a 1.7-kb Tn*1722* remnant together with an IS*26* element, and they displayed considerable modular diversification: i) a concise class 2 integron In2-16 with GCA *lnu*(F)*1b–dfrA1–aadA1a* in the MDR regions from T7RE$_{PROV087}$, T7RE$_{PROV023}$, and T7RE$_{MF1}$, while a complex In2-16 carrying VR1/GCA as

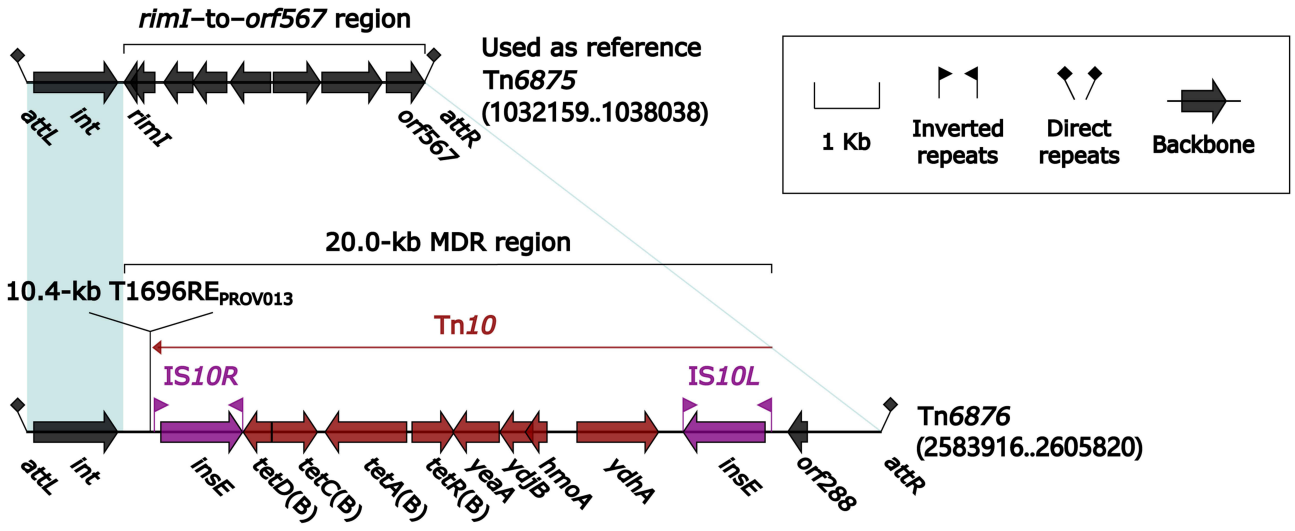

Figure 7 Comparison of two related IMEs Tn*6875* and Tn*6876*.
Notes: Genes are denoted by arrows. Genes, AGEs, and other features are colored based on their functional classification. Shading in light blue denotes regions of homology (nucleotide identity ≥95%). Numbers in brackets indicate nucleotide positions within the chromosomes of strains FDAARGOS_87 and PROV013, respectively. Accession number of Tn*6875* used as reference is CP031508.

above and additionally two copies of VR2 (IS*CR1–ble*$_{MBL}$–*bla*$_{NDM-1}$ unit) in the MDR region from T7RE$_{Pr-15-2-50}$; ii) a truncated IS*CR2–floR* unit, IS*CR2–sul2* unit, IS*26–aacC4–aph(4)-Ia*–IS*Ec59* unit, and a truncated *chrA–orf98* unit shared by the MDR regions from T7RE$_{PROV087}$ and T7RE$_{MF1}$; iii) a 71.2-kb Tn*21*-related element T21RE$_{PROV087}$ (see below) and a 21.2-kb T21RE$_{MF1}$ (see below) in the MDR regions from T7RE$_{PROV087}$ and T7RE$_{MF1}$, respectively; iv) IS*26–mph*(E)–IS*26* unit acquired by the MDR regions from T7RE$_{MF1}$ and T7RE$_{PROV023}$; v) intact or truncated Tn*4352* (containing *aphA1*) in the MDR regions from T7RE$_{MF1}$ and T7RE$_{Pr-15-2-50}$; vi) a complex class 1 integron In37 with four resistance loci: VR1/GCA (*aacA4cr–bla*$_{OXA-1}$*–catB3–arr-3*), a disrupted Tn*2* (containing *bla*$_{TEM-1}$), ΔTn*6502a* (containing *bla*$_{CTX-M-3}$), and VR2 (IS*CR1–rmtB* unit) in the MDR region from T7RE$_{PROV023}$; and vii) ΔTn*1548* carrying IS*CR1–armA* unit and an interrupted IS*Ec29–mph*(E)–IS*15DI* unit in the MDR region from T7RE$_{Pr-15-2-50}$.

*Three Tn*1696 *Derivatives Tn*6910, *T1696RE*$_{PROV002}$, *and T1696RE*$_{PROV013}$

Herein, a detailed sequence comparison (Figure 10) was applied to the three Tn*1696* derivatives Tn*6910*, T1696RE$_{PROV002}$, and T1696RE$_{PROV013}$ (identified as the inner components of Tn*6874*, Tn*6861*, and Tn*6876*, respectively; see above), together with Tn*1696*,[35] Tn*6338*,[36] and Tn*6909*[22] derived from GenBank. Tn*1696* was one of the Tn*3*-family prototype unit transposons, and it was originally found in plasmid R1003 from *Pseudomonas aeruginosa* and contained a core backbone structure: IRL (inverted repeat left)–*tnpA–tnpR* (resolvase)–*res* (resolution site)–*mer*–IRR (inverted repeat right).[35] These above five Tn*1696* derivatives exhibited three major modular differences cross the core backbones: i) an intact version of *tnpAR–res* in Tn*6338*, Tn*6909*, and Tn*6910*, while a truncated version in T1696RE$_{PROV002}$ and T1696RE$_{PROV013}$; ii) a Tn*1696 mer* locus in Tn*6338* and Tn*6910*, and a Tn*21 mer* locus instead in Tn*6909*; none of *mer* locus in T1696RE$_{PROV002}$ and T1696RE$_{PROV013}$; and iii) intact IRL/R in Tn*6910*, and IRL/R interrupted by insertion of IS*4321* in Tn*6909*; only IRL in T1696RE$_{PROV013}$, and IRL interrupted by insertion of IS*5075* in Tn*6338*; only IRR in Tn*6338*; none of IRL/R in T1696RE$_{PROV002}$.

Each of these five Tn*1696* derivatives acquired one or more integrons into *res* site, instead of In4 (GCA: *aacC1–gcuE–aadA2–cmlA1*) in Tn*1696*: a complex class 1 integron In469 in Tn*6338*, a different complex In469 in T1696RE$_{PROV002}$, a concise class 1 integron In27 (GCA: *dfrA12–gcuF–aadA2*) in T1696RE$_{PROV013}$, a distinct complex In27 in Tn*6909*, and the four tandem concise class 1 integrons including In1849 (GCA: *dfrA1t–aacA4'–bla*$_{OXA-1}$), two copies of In994 (GCA: *bla*$_{IMP-1}$), and In151 [GCA: *catB8–lnu*(F)*3*] in Tn*6910*. These two complex In469 harbored the same VR1/GCA (*arr-3–dfrA27–aadA16*), but differed from each other by capturing different additional VR modules: VR2 (IS*CR1–qnrB4–bla*$_{DHA-1}$ unit) in In469 from Tn*6338*, and VR2 (IS*CR1–bla*$_{PER-1}$ unit) together with VR3 (a truncated IS*CR1–aphA6* unit, ΔIS*Sod18*,

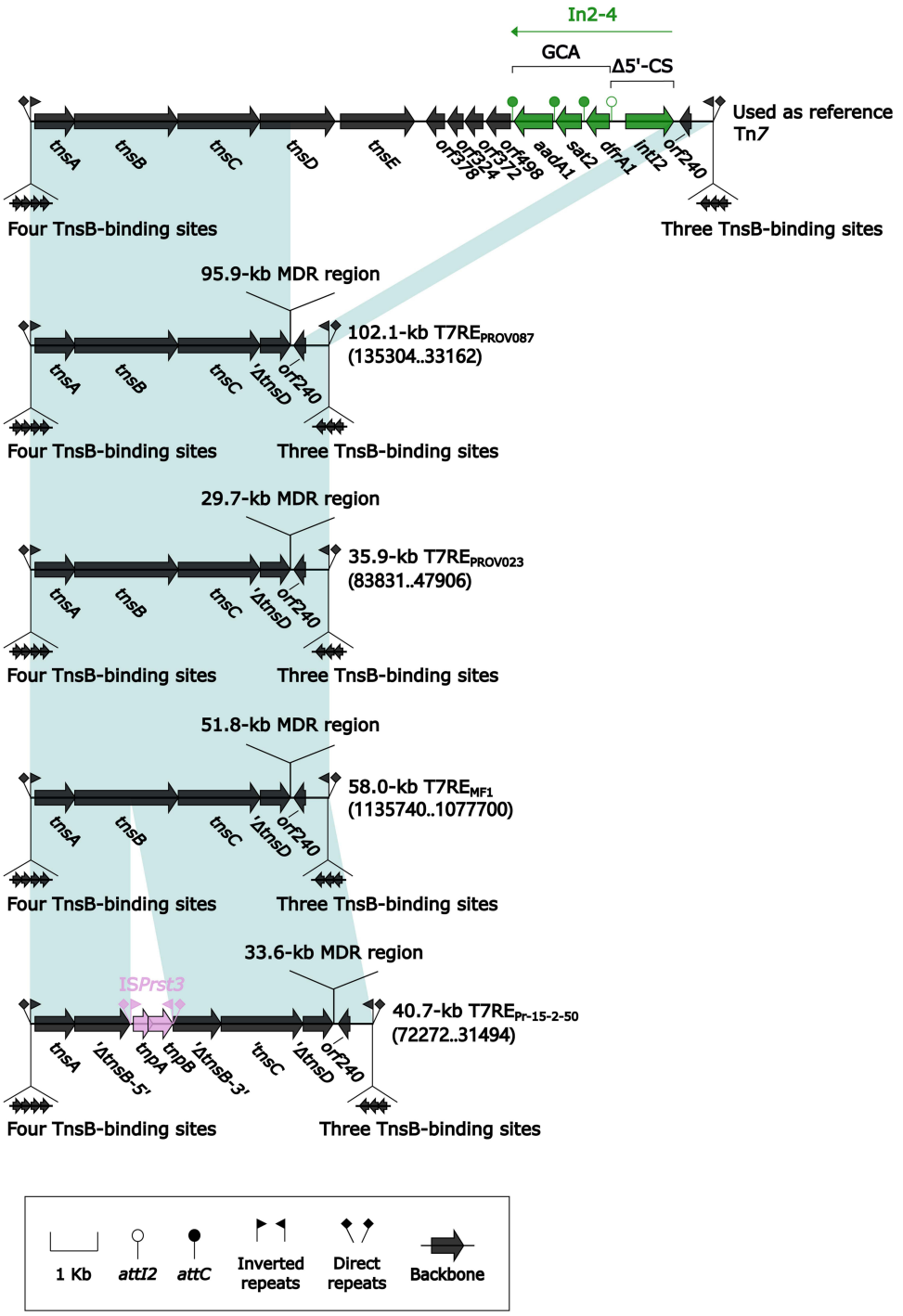

Figure 8 Comparison of Tn7 and its four derivatives.

Notes: Genes are denoted by arrows. Genes, AGEs, and other features are colored based on their functional classification. Shading in light blue denotes regions of homology (nucleotide identity ≥95%). Numbers in brackets indicate nucleotide positions within the chromosomes of strains PROV087, PROV023, MF1, and Pr-15-2-50, respectively. Accession number of Tn*7*[47] used as reference is KX117211.

and IS*Ec29*) in In469 from T1696RE$_{PROV002}$. The complex In27 from Tn*6909* carried GCA (VR1) as above and still captured four additional resistance modules: a truncated IS*CR1–qnrA1* unit (VR2), *chrA–orf98* unit, a truncated IS*26–mph* (A)–IS*6100* unit, and a concise class 1 integron In1209 (GCA: *aadA1b–dfrA1b–aacA7–bla*$_{VIM-1}$).

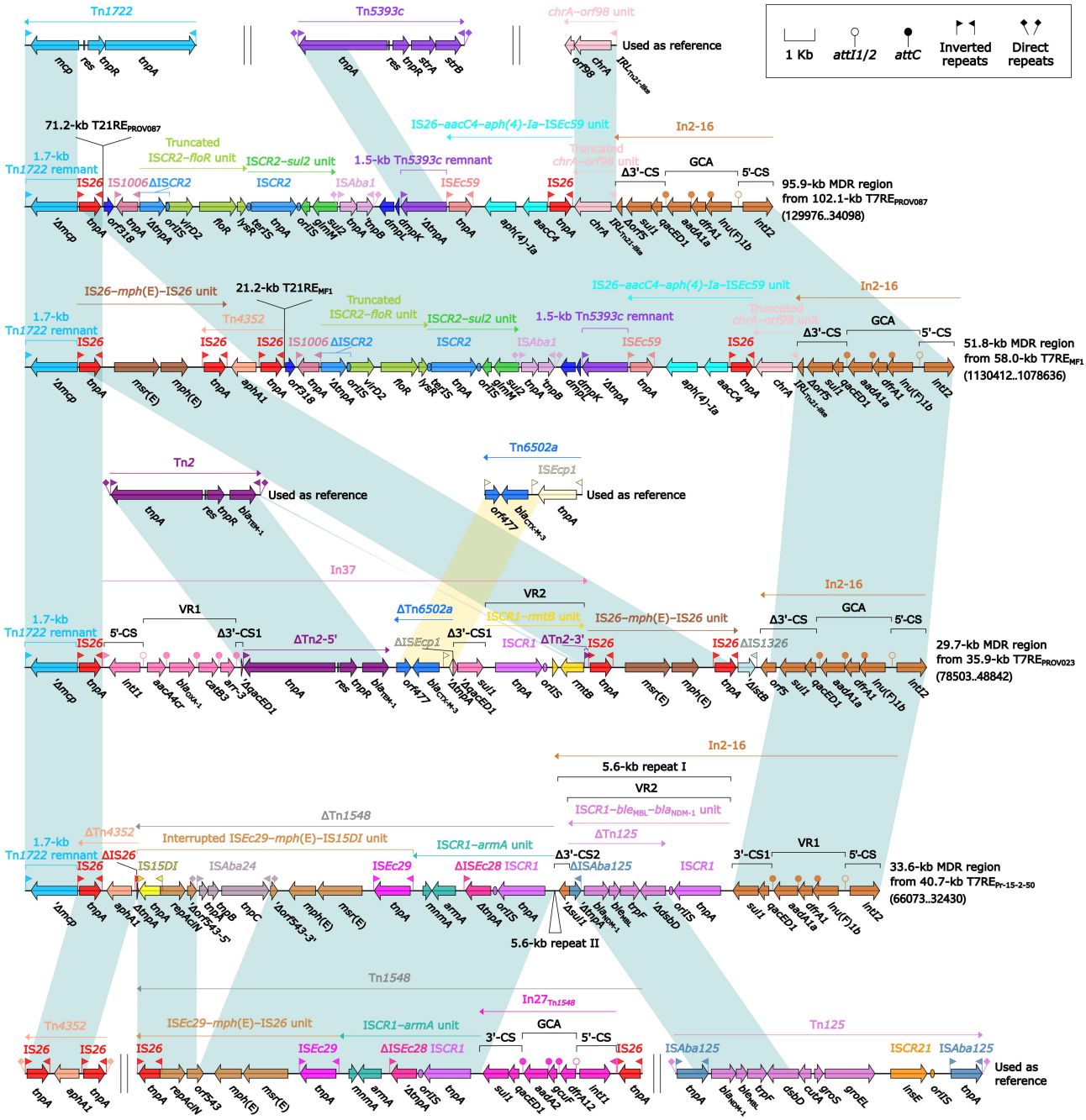

Figure 9 Comparison of MDR regions from four Tn7 derivatives.

Notes: Genes are denoted by arrows. Genes, AGEs, and other features are colored based on their functional classification. Shading in light blue or light orange denotes regions of homology (nucleotide identity ≥95%). Numbers in brackets indicate nucleotide positions within the chromosomes of strains PROV087, MF1, PROV023, and Pr-15-2-50, respectively. Accession numbers of Tn*1722*,[54] Tn*5393c*,[52] *chrA–orf98* unit,[22] Tn2,[55] Tn*6502a*,[50] Tn*4352*,[53] Tn*1548*,[56] and Tn*125*[57] used as reference are X61367, AF262622, CP042858, HM749967, KF914891, CP042858, AF550415, and JN872328, respectively.

Three Tn21 Derivatives Tn6974, T21RE$_{PROV087}$, and T21RE$_{MF1}$

Herein, a detailed sequence comparison (Figure 11) was applied to the three Tn*21* derivatives Tn*6974*, T21RE$_{PROV087}$, and T21RE$_{MF1}$ (identified as the inner components of Tn*6873*, T7RE$_{PROV087}$, and T7RE$_{MF1}$, respectively; see above), together with Tn*21*[35] and Tn*6975*[37] derived from GenBank. Tn*21* was another prototype of Tn*3*-family unit transposons, and it was initially found in *Shigella flexneri* plasmid R100 and had a core backbone structure: IRL–*tnpA–tnpR–res–mer–*IRR.[35] The above four Tn*21* derivatives shared Tn*21 tnpAR–res*, but their backbones had at least two major modular

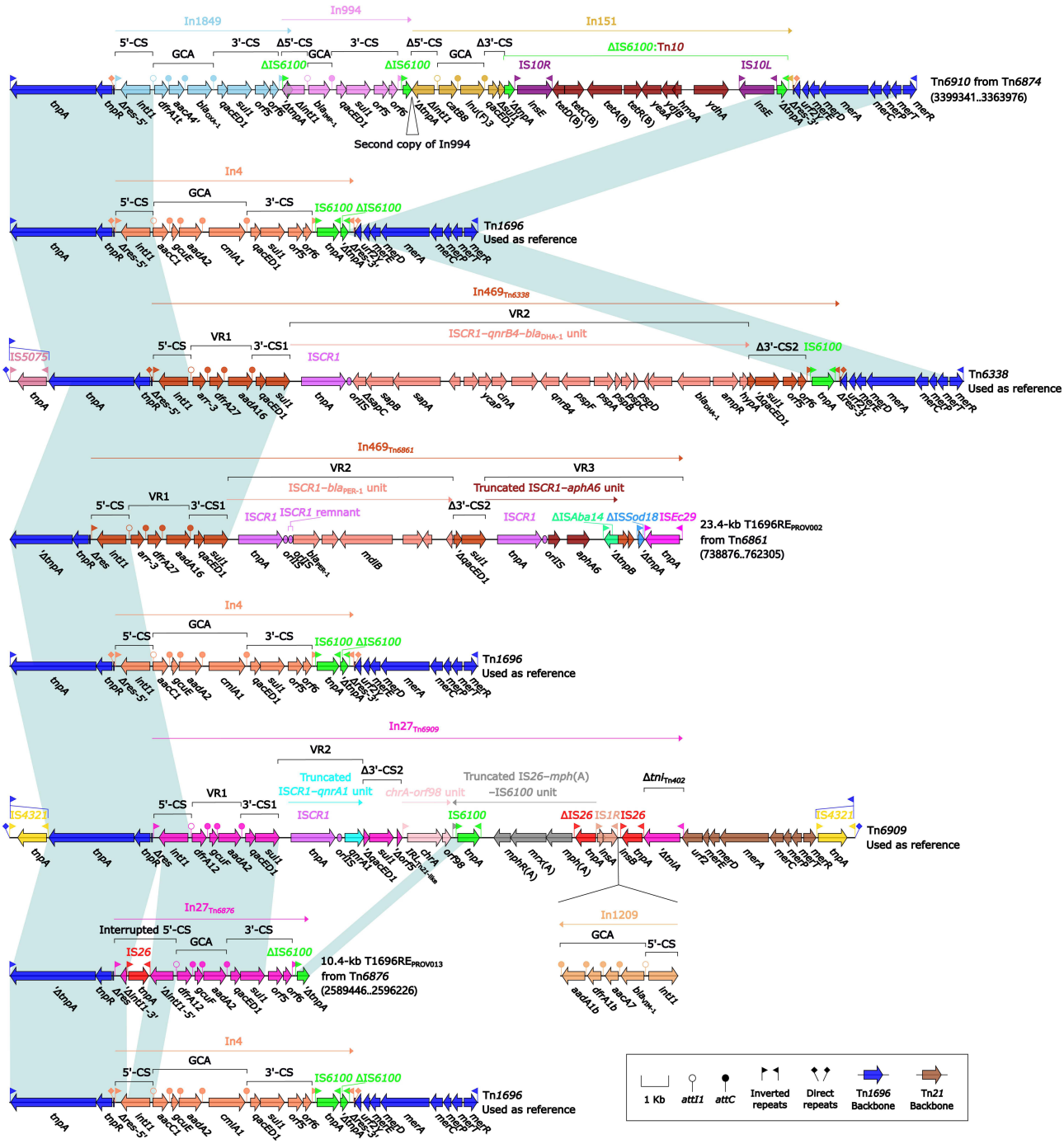

Figure 10 Comparison of Tn*1696* and its three derivatives.

Notes: Genes are denoted by arrows. Genes, AGEs, and other features are colored based on their functional classification. Shading in light blue denotes regions of homology (nucleotide identity ≥95%). Numbers in brackets indicate nucleotide positions within the chromosomes of strains BML2496, PROV002, and PROV013, respectively. Accession numbers of Tn*1696*,[35] Tn*6338*,[36] and Tn*6909*[22] used as reference are U12338, KY270853, and CP032168, respectively.

differences: i) a Tn*21 mer* locus in Tn*6975*, and a Tn*1696 mer* locus instead in Tn*6974*; none of *mer* locus in $T21RE_{MF1}$ and $T21RE_{PROV087}$; and ii) IRL/R in Tn*6974* and Tn*6975*, while only IRL in $T21RE_{PROV087}$ and $T21RE_{MF1}$.

Each of these four Tn*21* derivatives acquired an integron instead of In2 (GCA: *aadA1a*) in Tn*21*: a concise class 1 integron In1808 (GCA: *aacA4cr–bla*$_{OXA-1}$*–ΔcatB3–arr-3–dfrA27–aadA16*) in Tn*6974*, a concise class 1 integron In27 in Tn*6975*, a distinct complex In27 in $T21RE_{MF1}$, and a complex class 1 integron In263 in $T21RE_{PROV087}$. The concise In27 contained three resistance loci: *dfrA12–gcuF–aadA2* (GCA), *chrA–orf98* unit, and IS*26–mph*(A)–IS*6100* unit. The

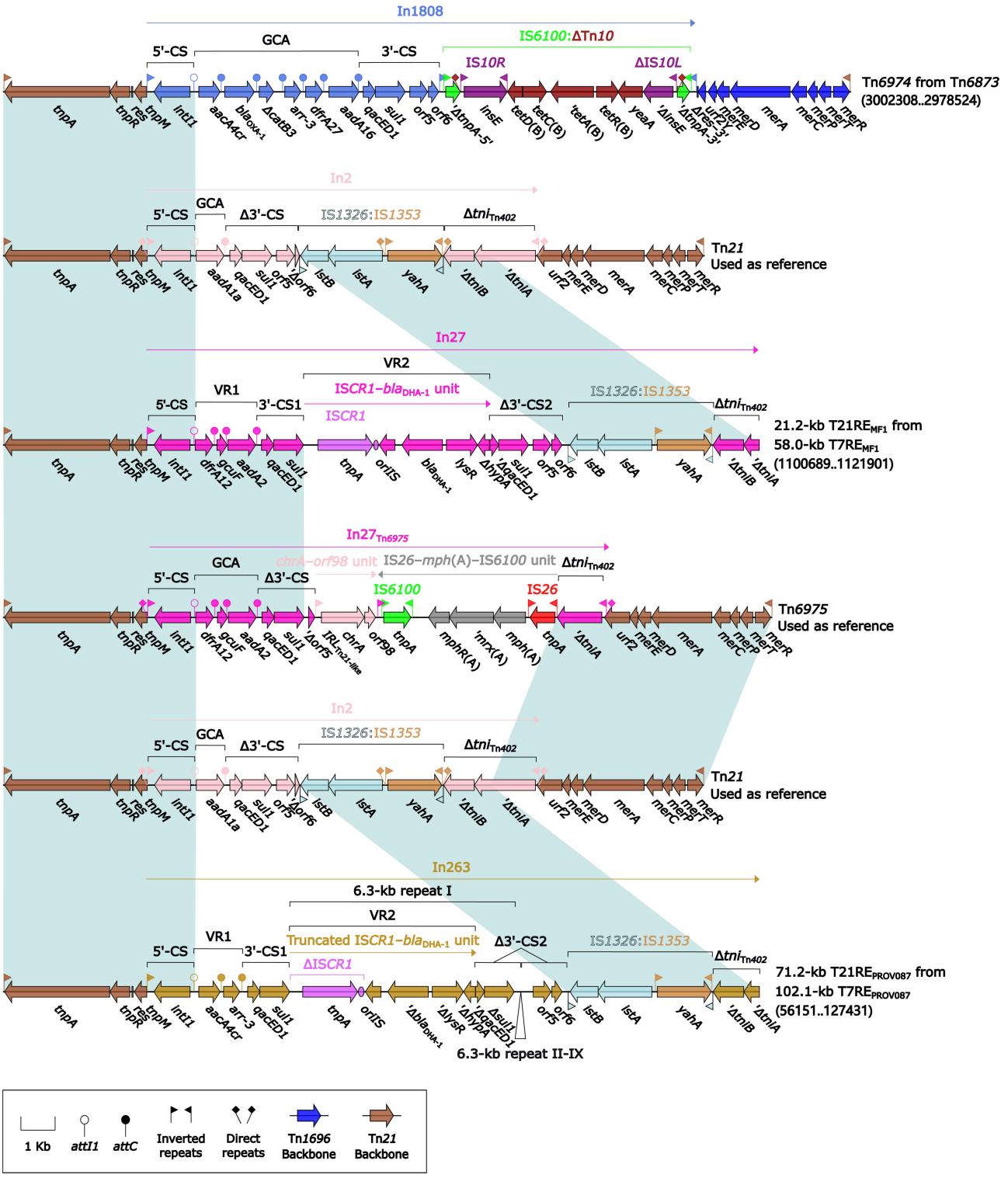

Figure 11 Comparison of Tn*21* and its three derivatives.

Notes: Genes are denoted by arrows. Genes, AGEs, and other features are colored based on their functional classification. Shading in light blue denotes regions of homology (nucleotide identity ≥95%). Numbers in brackets indicate nucleotide positions within the chromosomes of strains PROV013, MF1, and PROV087, respectively. Accession numbers of Tn*21*[35] and Tn*6975*[37] used as reference are AF071413 and CP041301, respectively.

complex In27 possessed a VR1/GCA as above and further acquired a VR2 (IS*CR1–bla*$_{DHA-1}$ unit). The complex In263 had a VR1/GCA (*aacA4cr–arr-3*) and additionally nine copies of VR2 (truncated IS*CR1–bla*$_{DHA-1}$ unit).

Transferability and Antimicrobial Susceptibility

Tn*6862*, which was selected to represent Tn*6512*-related ICEs, could be transferred from the wild-type PROV023 isolate into *E. coli* EC600 through conjugation, generating the transconjugant EC600/Tn*6862*. Both PROV023 and EC600/Tn*6862* were highly resistant to amikacin with a minimum inhibitory concentration (MIC) value ≥64 μg/mL (Table S3) owing to production of aminoglycoside 3'-phosphotransferase.

Plasmids in the Five Isolates Sequenced in This Study

Providencia rettgeri PROV087 and *Providencia alcalifaciens* PROV023 carried no plasmids. Identified were an IncC plasmid pPROV275-1NDM (carrying *bla*$_{NDM-1}$, *bla*$_{CMY-6}$, *aacA4, rmtC, sul1*, and *qacED1*), an Inc$_{pGZH766-NDM}$ plasmid pPROV275-2NDM (having *bla*$_{NDM-1}$, *bla*$_{PER-4}$, *bla*$_{OXA-10}$, *aadA1, aadB, aphA6, catA1, catB8, sul1*, and *qacED1*) together with a Col3M plasmid pPROV275-qnrD (containing *qnrD1*) in *Providencia rettgeri* PROV275, an IncW plasmid pPROV002-IMP (carrying *bla*$_{IMP-4}$, *bla*$_{NDM-1}$, *aacA4, catB3, sul1*, and *qacED1*) in *Providencia rettgeri* PROV002, and an Inc$_{pGZH766-NDM}$ plasmid pPROV013-PER [containing *bla*$_{PER-4}$, *bla*$_{OXA-1}$, *aacA4, mph*(E), *msr*(E), *arr-3, catB3, lnu*(G), *sul1*, and *qacED1*] together with an IncFII plasmid pPROV013-NR (harboring no resistance genes) in *Providencia alcalifaciens* PROV013.

Discussion

This work presents the complete sequences of seven chromosomal AGEs in *Providencia*, and they can be further divided into four groups: three Tn*6512*-related ICEs Tn*6860*, Tn*6861*, and Tn*6862*; one Tn*6872*-related IME Tn*6873*; one Tn*6875*-related IME Tn*6876*; and two Tn*7*-related elements T7RE$_{PROV087}$ and T7RE$_{PROV023}$. Newly identified are five (except for T7RE$_{PROV087}$ and T7RE$_{PROV023}$) of the above seven AGEs, together with one unit transposon Tn*6974*, one composite transposon Tn*6976*, and two integrons In1793 and In1808, all of which are located within these five AGEs. There are additional 10 newly designated (firstly designated in this study, but with previously determined sequences) AGEs: i) one IME Tn*6912* located within Tn*6860* sequenced in this study; ii) one ICEs Tn*6865*, four IMEs Tn*6872*, Tn*6874*, Tn*6875*, and Tn*6977*, two unit transposons Tn*6910* and Tn*6975*, one composite transposon Tn*6896*, and one IS element IS*Prre11* which come from GenBank and are included in the sequence comparison herein. This is also the first report of identifying Tn*6872* and Tn*6875* in *Providencia*. The two previously designated ICEs ICE*Pal*Ban1 and ICE*Pre*ChnRF14-2 were renamed herein as standard Tn designations Tn*6863* and Tn*6864*, respectively.

The transposition of Tn*7*-related unit transposons, generating bracketed 5-bp DRs, is generally site-specific at 25-bp downstream of *glmS*, and these target sites with a consensus CCgcGtAAccTgGCaAAatcgGTtACgGTtGAgTaa[38] together with Tn*7*-related elements are presented in a wide range of bacteria as mentioned above. Three of the four Tn*7*-related elements (all bracketed by 5-bp DRs) characterized herein, as expected, are located downstream of *glmS*, but T7RE$_{MF1}$ is presented within *orf1389*. The presence of bracketed 5-bp DRs denotes that T7RE$_{MF1}$ is most likely transposed directly into *orf1389* that does not contain the above consensus target site; similarly, additional target sites, not resembling that downstream of *glmS*, have been proposed previously for integration of Tn*7*-related unit transposons.[25] Tn*6512*-related ICEs have 17-bp highly conserved *attP* (attachment site on the ICE) sequences with a consensus ATcATcTCtCACCCtGA. Integration of these ICEs needs the 17-bp relatively non-conserved *attB* (attachment site on the chromosome) target sites within the 5' end of *prfC*,[32] and can occur with up to 23.5% sequence mismatch between *attB* and *attP*.[39] These *attB* sites together with Tn*6512*-related ICEs are widely distributed in Gram-negative bacteria as mentioned above. Taken together, Tn*7*-related unit transposons and Tn*6512*-related ICEs have a wide host range.

Conjugal transfer experiments confirm that Tn*6512*-related ICEs with the complete gene sets for conjugal transfer have the ability to transfer from the wild-type isolates of *Proteus*,[40] *Vibrio*,[41] *Shewanella*,[42] and *Providencia* (this study) to the recipient bacteria *E. coli*, and that a circular extrachromosomal Tn*6512* has the ability to transfer into the recipient bacteria *Salmonella*,[39] *Enterobacter*,[39] and *Serratia*,[39] indicating that this group of ICEs have a very broad host range.

Integration of T*n6872*-related IMEs needs 24-bp highly conserved *attB* sequences (with a consensus AACCTAcAaTTtAACCTACACTTA) located 102-bp upstream of *mutS*. These *attB* sequences together with Tn*6872*-related elements are mainly found in Morganellaceae including *Providencia* (this study), *Proteus* (eg *Proteus mirabilis* with an accession number CP053894), and Morganella (eg *M. morganii* with an accession number CP064830). Integration of Tn*6875*-related IMEs recognizes 11-bp highly conserved *attB* sequences (with a consensus CcTatTTTATC) located 494-bp downstream of *smpB*. These *attB* sites together with Tn*6875*-related elements are mainly distributed in Morganellaceae including *Providencia* (this study), *Proteus* (eg *Proteus mirabilis* with an accession number CP042857), and *Morganella* (eg *M. morganii* with an accession number CP068145), as well as Enterobacteriaceae including *Salmonella* (eg *S. enterica* with an accession number CP053319) and *Escherichia* (eg *E. coli* with an accession number CP056565). It seems that these two groups of IMEs spread mainly in Morganellaceae and/or Enterobacteriaceae.

Five (except for Tn*6862* and Tn*6865*) of the seven Tn*6512*-related ICEs encode the toxin-antitoxin systems: HipBA in Tn*6512*, and AbiEi-ii in Tn*6860*, Tn*6861*, Tn*6863*, and Tn*6864*. These toxin-antitoxin systems have been shown to stabilize Tn*6512*-related ICEs by preventing their loss when they are extrachromosomal.[43,44] The loss of the AbiEi-ii toxin-antitoxin system from Tn*6512* and Tn*6862* is due to the substitution of ICE backbone region 7 as shown in Figure 2, while that from Tn*6865* is caused by the insertion of the MDR region within the ICE backbone gene *umuC* (site 3 in Figure 2). Five (except for Tn*6512* and Tn*6865*) of the seven Tn*6512*-related ICEs and two (except for Tn*6872*) of the three Tn*6872*-related IMEs carry a type I restriction-modification system HsdMSR. This system can degrade the unmethylated incoming DNA to stabilize AGEs against challenges by competitor elements.[45] Tn*6512* lose the HsdMSR system because of the substitution of backbones region 5 (Figure 2). The loss of this system from Tn*6865* is on account of the insertion of the MDR region. Tn*6872* do not harbor this system due the substitution of *orf201*–to–*orf207* region (Figure 5). It is speculated herein that the loss of toxin-antitoxin or restriction-modification systems might lead to the instability of relevant ICEs and IMEs after they are excised from the chromosomes.[46]

Tn*7*-related unit transposons accomplish transposition using the core transposition module *tnsABCDE*.[23] All the four Tn*7*-related elements analyzed herein have undergone the truncation of *tnsABCDE*, which results from the integration of MDR regions. The lesion of *tnsABCDE* in these four Tn*7*-related elements would lose their ability of intracellular transfer.

Each of 13 of the totally characterized 17 AGEs carries a MDR region, and notably the resulting 13 MDR regions carry at least 49 drug resistance genes, which can be grouped into 15 different categories of antimicrobials and heavy metal, including β-lactam, aminoglycoside, macrolide, tetracycline, trimethoprim, phenicol, sulphonamide, lincosamide, rifampicin, quinolone, fosfomycin, bleomycin, chromate, quaternary ammonium compound, and mercury. Among these 49 drug resistance genes, predominantly found are those resistant to aminoglycosides (n=14) and β-lactams (n=9), which might be due to the wide clinical use of aminoglycosides and β-lactams against *Providencia*-induced infections. Intact or truncated versions of Tn*21*- and Tn*1696*-related transposons, Tn*4352*, Tn*5393c*, In27, IS*CR2*–*floR* unit, IS*CR2*–*sul2* unit, IS*Ec29*–*mph*(E)–IS*15DI* unit, and IS*26*–*aacC4*–*aph(4)-Ia*–IS*Ec59* unit are frequently found within these 13 MDR regions, indicating the assembly of these MDR regions from various collections of AGEs and associated resistance genes via complex transposition and homologous recombination. In addition, there are so called "concise" accessory modules (Tn*6912*, Tn*6578*, Tn*6896*, In2-4, In9-1, and *mer* region) that are presented in six AGEs, including four harboring MDR regions and two not. These "concise" accessory modules harbor at least 10 drug resistance genes, which mediate the resistance to six different categories of antimicrobials and heavy metal, including aminoglycoside, β-lactam, tetracycline, trimethoprim, macrolide, and mercury.

On the one hand, these four groups of AGEs have a wide range of hosts including *Providencia*, and they are stable in the host bacteria and further able to transfer across different bacterial species. On the other hand, these four groups of AGEs display high-level diversification in modular structures, which have complex mosaic natures and carry a large number of drug resistance genes, and particularly different MDR regions are presented in these AGEs. Integration of these AGEs into the *Providencia* chromosomes contributes to the accumulation and distribution of drug resistance genes and enhances the ability of *Providencia* isolates to survive under drug selection pressure.

Data Sharing Statement

The complete chromosome sequences of the PROV275, PROV002, PROV023, PROV013, and PROV087 isolates were submitted to GenBank under accession numbers CP059298, CP059345, CP059348, CP059346, and CP059347, respectively. The GenBank accession numbers of all the six plasmids of these five isolates were listed in Table S1.

Ethics Statement

This study used the bacterial isolates obtained from the Chinese public hospitals as listed in Table S1. The bacterial isolation was part of the routine hospital laboratory procedures and the bacterial isolates involved in this study were not isolated from patients directly. The genetic analysis of accessory genetic elements in this study had no experimentation involving humans or animals. According to relevant legislation/policy of China (http://www.nhc.gov.cn/fzs/s3576/201808/14ee8ab2388440c4a44ecce0f24e064c.shtml), this study was not subject to ethical review. The research involving biohazards and all related procedures were approved by the Biosafety Committee of the Beijing Institute of Microbiology and Epidemiology.

Acknowledgments

All experiments and data analyses were done in Dr. Dongsheng Zhou's laboratory.

Funding

This research was funded by the National Key Research and Development Program of China under Grant 2016YFD0501305.

Disclosure

The authors report no conflicts of interest in this work.

References

1. O'Hara CM, Brenner FW, Miller JM. Classification, identification, and clinical significance of *Proteus, Providencia*, and *Morganella*. *Clin Microbiol Rev*. 2000;13(4):534–546. doi:10.1128/CMR.13.4.534
2. Stock I, Wiedemann B. Natural antibiotic susceptibility of *Providencia stuartii, P. rettgeri, P. alcalifaciens* and *P. rustigianii* strains. *J Med Microbiol*. 1998;47(7):629–642. doi:10.1099/00222615-47-7-629
3. Swiatlo E, Kocka FE. Inducible expression of an aminoglycoside-acetylating enzyme in *Providencia stuartii*. *J Antimicrob Chemother*. 1987;19(1):27–30. doi:10.1093/jac/19.1.27
4. Yaghoubi S, Zekiy AO, Krutova M, et al. Tigecycline antibacterial activity, clinical effectiveness, and mechanisms and epidemiology of resistance: narrative review. *Eur J Clin Microbiol Infect Dis*. 2021;1:1–20.
5. Samonis G, Korbila IP, Maraki S, et al. Trends of isolation of intrinsically resistant to colistin Enterobacteriaceae and association with colistin use in a tertiary hospital. *Eur J Clin Microbiol Infect Dis*. 2014;33(9):1505–1510. doi:10.1007/s10096-014-2097-8
6. Munita JM, Arias CA. Mechanisms of antibiotic resistance. *Microbiol Spectr*. 2016;4(2):10. doi:10.1128/microbiolspec.VMBF-0016-2015
7. Johnson CM, Grossman AD. Integrative and conjugative elements (ICEs): what they do and how they work. *Annu Rev Genet*. 2015;49(1):577–601. doi:10.1146/annurev-genet-112414-055018
8. Coetzee JN, Datta N, Hedges RW. R factors from *Proteus rettgeri*. *J Gen Microbiol*. 1972;72(3):543–552. doi:10.1099/00221287-72-3-543
9. Olaitan AO, Diene SM, Assous MV, Rolain J-M. Genomic plasticity of multidrug-resistant NDM-1 positive clinical isolate of *Providencia rettgeri*. *Genome Biol Evol*. 2016;8(3):723–728. doi:10.1093/gbe/evv195
10. Flannery EL, Mody L, Mobley HLT. Identification of a modular pathogenicity island that is widespread among urease-producing uropathogens and shares features with a diverse group of mobile elements. *Infect Immun*. 2009;77(11):4887–4894. doi:10.1128/IAI.00705-09
11. Li R, Lu X, Peng K, et al. Deciphering the structural diversity and classification of the mobile tigecycline resistance gene *tet*(X)-bearing plasmidome among bacteria. *mSystems*. 2020;5(2):e00134–e00120. doi:10.1128/mSystems.00134-20
12. Ryan MP, Armshaw P, O'Halloran JA, Pembroke JT. Analysis and comparative genomics of R997, the first SXT/R391 integrative and conjugative element (ICE) of the Indian Sub-Continent. *Sci Rep*. 2017;7(1):8562. doi:10.1038/s41598-017-08735-y
13. Taviani E, Ceccarelli D, Lazaro N, et al. Environmental *Vibrio* spp., isolated in Mozambique, contain a polymorphic group of integrative conjugative elements and class 1 integrons. *FEMS Microbiol Ecol*. 2008;64(1):45–54. doi:10.1111/j.1574-6941.2008.00455.x
14. Pembroke JT, Piterina AV. A novel ICE in the genome of *Shewanella putrefaciens* W3-18-1: comparison with the SXT/R391 ICE-like elements. *FEMS Microbiol Lett*. 2006;264(1):80–88. doi:10.1111/j.1574-6968.2006.00452.x
15. Xu J, Jia H, Cui G, et al. ICE*Apl*Chn1, a novel SXT/R391 integrative conjugative element (ICE), carrying multiple antibiotic resistance genes in *Actinobacillus pleuropneumoniae*. *Vet Microbiol*. 2018;220:18–23. doi:10.1016/j.vetmic.2018.05.002
16. López-Pérez M, Gonzaga A, Rodriguez-Valera F. Genomic diversity of "deep ecotype" *Alteromonas macleodii* isolates: evidence for Pan-Mediterranean clonal frames. *Genome Biol Evol*. 2013;5(6):1220–1232. doi:10.1093/gbe/evt089

17. Wang H, Sun B, Xie G, Wan X, Huang J, Song X. Spotlight on a novel bactericidal mechanism and a novel SXT/R391-like integrative and conjugative element, carrying multiple antibiotic resistance genes, in *Pseudoalteromonas flavipulchra* strain CDM8. *Microbiol Res*. 2021;242:126598. doi:10.1016/j.micres.2020.126598
18. Wozniak RAF, Fouts DE, Spagnoletti M, et al. Comparative ICE genomics: insights into the evolution of the SXT/R391 family of ICEs. *PLoS Genet*. 2009;5(12):e1000786. doi:10.1371/journal.pgen.1000786
19. Guedon G, Libante V, Coluzzi C, Payot S, Leblond-Bourget N. The obscure world of integrative and mobilizable elements, highly widespread elements that pirate bacterial conjugative systems. *Genes*. 2017;8(11):337. doi:10.3390/genes8110337
20. Carraro N, Rivard N, Ceccarelli D, Colwell RR, Burrus V. IncA/C conjugative plasmids mobilize a new family of multidrug resistance islands in clinical *Vibrio cholerae* Non-O1/Non-O139 isolates from Haiti. *mBio*. 2016;7(4):e00509–e00516. doi:10.1128/mBio.00509-16
21. Soliman AM, Shimamoto T, Nariya H, Shimamoto T. Emergence of *Salmonella* genomic island 1 variant SGI1-W in a clinical isolate of *Providencia stuartii* from Egypt. *Antimicrob Agents Chemother*. 2019;63(1):e01793–e01718. doi:10.1128/AAC.01793-18
22. Luo X, Yin Z, Zeng L, et al. Chromosomal integration of huge and complex bla_{NDM}-carrying genetic elements in Enterobacteriaceae. *Front Cell Infect Microbiol*. 2021;11:690799. doi:10.3389/fcimb.2021.690799
23. Peters JE. Targeted transposition with Tn*7* elements: safe sites, mobile plasmids, CRISPR/Cas and beyond. *Mol Microbiol*. 2019;112 (6):1635–1644. doi:10.1111/mmi.14383
24. Parks AR, Peters JE. Transposon Tn*7* is widespread in diverse bacteria and forms genomic islands. *J Bacteriol*. 2007;189(5):2170–2173. doi:10.1128/JB.01536-06
25. Ramírez MS, Piñeiro S, Centrón D. Novel insights about class 2 integrons from experimental and genomic epidemiology. *Antimicrob Agents Chemother*. 2010;54(2):699–706. doi:10.1128/AAC.01392-08
26. Zhang Y, Cao Y, Zhang L, Hikichi Y, Ohnishi K, The LJ. Tn*7*-based genomic integration is dependent on an *att*Tn*7* box in the *glmS* gene and is site-specific with monocopy in *Ralstonia solanacearum* species complex. *Mol Plant Microbe Interact*. 2021;34(7):720–725. doi:10.1094/MPMI-11-20-0325-SC
27. Ramírez MS, Quiroga C, Centrón D. Novel rearrangement of a class 2 integron in two non-epidemiologically related isolates of *Acinetobacter baumannii*. *Antimicrob Agents Chemother*. 2005;49(12):5179–5181. doi:10.1128/AAC.49.12.5179-5181.2005
28. Fu J, Zhang J, Yang L, et al. Precision methylome and *in vivo* methylation kinetics characterization of *Klebsiella Pneumoniae*. *Genom Proteom Bioinform*. 2021. doi:10.1016/j.gpb.2021.04.002
29. De Coster W, D'Hert S, Schultz DT, Cruts M, Van Broeckhoven C. NanoPack: visualizing and processing long-read sequencing data. *Bioinformatics*. 2018;34(15):2666–2669. doi:10.1093/bioinformatics/bty149
30. Qu D, Shen Y, Hu L, et al. Comparative analysis of KPC-2-encoding chimera plasmids with multi-replicon IncR:$Inc_{pA1763\text{-}KPC}$:IncN1 or $IncFII_{pHN7A8}$:$Inc_{pA1763\text{-}KPC}$:IncN1. *Infect Drug Resist*. 2019;12:285–296. doi:10.2147/IDR.S189168
31. CLSI. CLSI supplement M100. In: *Performance Standards for Antimicrobial Susceptibility Testing*. 30th ed. Wayne, PA: Clinical and Laboratory Standards Institute; 2020.
32. Hochhut B, Beaber JW, Woodgate R, Waldor MK. Formation of chromosomal tandem arrays of the SXT element and R391, two conjugative chromosomally integrating elements that share an attachment site. *J Bacteriol*. 2001;183(4):1124–1132. doi:10.1128/JB.183.4.1124-1132.2001
33. Botelho J, Schulenburg H. The role of integrative and conjugative elements in antibiotic resistance evolution. *Trends Microbiol*. 2021;29(1):8–18. doi:10.1016/j.tim.2020.05.011
34. Carattoli A, Seiffert SN, Schwendener S, Perreten V, Endimiani A. Differentiation of IncL and IncM plasmids associated with the spread of clinically relevant antimicrobial resistance. *PLoS One*. 2015;10(5):e0123063. doi:10.1371/journal.pone.0123063
35. Partridge SR, Brown HJ, Stokes HW, Hall RM. Transposons Tn*1696* and Tn*21* and their integrons In4 and In2 have independent origins. *Antimicrob Agents Chemother*. 2001;45(4):1263–1270. doi:10.1128/AAC.45.4.1263-1270.2001
36. Liang Q, Jiang X, Hu L, et al. Sequencing and genomic diversity analysis of IncHI5 plasmids. *Front Microbiol*. 2018;9:3318. doi:10.3389/fmicb.2018.03318
37. Desloges I, Taylor JA, Leclerc J-M, et al. Identification and characterization of OmpT-like proteases in uropathogenic *Escherichia coli* clinical isolates. *MicrobiologyOpen*. 2019;8(11):e915. doi:10.1002/mbo3.915
38. Mitra R, McKenzie GJ, Yi L, Lee CA, Craig NL. Characterization of the TnsD-*att*Tn*7* complex that promotes site-specific insertion of Tn*7*. *Mob DNA*. 2010;1(1):18. doi:10.1186/1759-8753-1-18
39. McGrath BM, Pembroke JT. Detailed analysis of the insertion site of the mobile elements R997, pMERPH, R392, R705 and R391 in *E. coli* K12. *FEMS Microbiol Lett*. 2004;237(1):19–26. doi:10.1111/j.1574-6968.2004.tb09673.x
40. Li X, Du Y, Du P, et al. SXT/R391 integrative and conjugative elements in *Proteus* species reveal abundant genetic diversity and multidrug resistance. *Sci Rep*. 2016;6:37372. doi:10.1038/srep37372
41. Sarkar A, Morita D, Ghosh A, et al. Altered integrative and conjugative elements (ICEs) in recent *Vibrio cholerae* O1 isolated from cholera cases, Kolkata, India. *Front Microbiol*. 2019;10:2072. doi:10.3389/fmicb.2019.02072
42. Fang Y, Wang Y, Li Z, et al. Distribution and genetic characteristics of SXT/R391 integrative conjugative elements in *Shewanella* spp. from China. *Front Microbiol*. 2018;9:920. doi:10.3389/fmicb.2018.00920
43. Carraro N, Poulin D, Burrus V. Replication and active partition of integrative and conjugative elements (ICEs) of the SXT/R391 family: the line between ICEs and conjugative plasmids is getting thinner. *PLoS Genet*. 2015;11(6):e1005298. doi:10.1371/journal.pgen.1005298
44. Wozniak RAF, Waldor MK. A toxin-antitoxin system promotes the maintenance of an integrative conjugative element. *PLoS Genet*. 2009;5(3): e1000439. doi:10.1371/journal.pgen.1000439
45. Oliveira PH, Touchon M, Rocha EPC. The interplay of restriction-modification systems with mobile genetic elements and their prokaryotic hosts. *Nucleic Acids Res*. 2014;42(16):10618–10631. doi:10.1093/nar/gku734
46. Huguet KT, Gonnet M, Doublet B, Cloeckaert A. A toxin antitoxin system promotes the maintenance of the IncA/C-mobilizable *Salmonella* genomic island 1. *Sci Rep*. 2016;6(1):32285. doi:10.1038/srep32285
47. Peters JE, Craig NL. Tn*7*: smarter than we thought. *Nat Rev Mol Cell Biol*. 2001;2(11):806–814. doi:10.1038/35099006
48. Sun F, Zhou D, Sun Q, et al. Genetic characterization of two fully sequenced multi-drug resistant plasmids pP10164-2 and pP10164-3 from *Leclercia adecarboxylata*. *Sci Rep*. 2016;6(1):33982. doi:10.1038/srep33982

49. Xie L, Wu J, Zhang F, et al. Molecular epidemiology and genetic characteristics of various *bla*$_{PER}$ genes in Shanghai, China. *Antimicrob Agents Chemother*. 2016;60(6):3849–3853. doi:10.1128/AAC.00258-16
50. Chen L, Hu H, Chavda KD, et al. Complete sequence of a KPC-producing IncN multidrug-resistant plasmid from an epidemic *Escherichia coli* sequence type 131 strain in China. *Antimicrob Agents Chemother*. 2014;58(4):2422–2425. doi:10.1128/AAC.02587-13
51. Stanisich VA, Bennett PM, Richmond MH. Characterization of a translocation unit encoding resistance to mercuric ions that occurs on a nonconjugative plasmid in *Pseudomonas aeruginosa*. *J Bacteriol*. 1977;129(3):1227–1233. doi:10.1128/jb.129.3.1227-1233.1977
52. L'Abée-Lund TM, Sørum H. Functional Tn*5393*-like transposon in the R plasmid pRAS2 from the fish pathogen *Aeromonas salmonicida* subspecies *Salmonicida* isolated in Norway. *Appl Environ Microbiol*. 2000;66(12):5533–5535. doi:10.1128/AEM.66.12.5533-5535.2000
53. Wrighton CJ, Strike P. A pathway for the evolution of the plasmid NTP16 involving the novel kanamycin resistance transposon Tn*4352*. *Plasmid*. 1987;17(1):37–45. doi:10.1016/0147-619X(87)90006-0
54. Wang L, Fang H, Feng J, et al. Complete sequences of KPC-2-encoding plasmid p628-KPC and CTX-M-55-encoding p628-CTXM coexisted in *Klebsiella pneumoniae*. *Front Microbiol*. 2015;6:838. doi:10.3389/fmicb.2015.00838
55. Heffron F, Sublett R, Hedges RW, Jacob A, Falkow S. Origin of the TEM-beta-lactamase gene found on plasmids. *J Bacteriol*. 1975;122 (1):250–256. doi:10.1128/jb.122.1.250-256.1975
56. Galimand M, Sabtcheva S, Courvalin P, Lambert T. Worldwide disseminated *armA* aminoglycoside resistance methylase gene is borne by composite transposon Tn*1548*. *Antimicrob Agents Chemother*. 2005;49(7):2949–2953. doi:10.1128/AAC.49.7.2949-2953.2005
57. Poirel L, Bonnin RA, Boulanger A, Schrenzel J, Kaase M, Nordmann P. Tn*125*-related acquisition of *bla*$_{NDM}$-like genes in *Acinetobacter baumannii*. *Antimicrob Agents Chemother*. 2012;56(2):1087–1089. doi:10.1128/AAC.05620-11